Journal of Alloys and Compounds 509S (2011) S839–S843

Contents lists available at ScienceDirect

Journal of Alloys and Compounds

journal homepage: www.elsevier.com/locate/jallcom

IMC hydrides with high hydrogen dissociation pressure

T.A. Zotov[a,*], R.B. Sivov[b], E.A. Movlaev[a], S.V. Mitrokhin[a], V.N. Verbetsky[a]

[a] Chemistry Department, Lomonosov Moscow State University, Leninskie Gory 1-3, Moscow 119991, Russia
[b] Department of Material Science, Lomonosov Moscow State University, Leninskie Gory 1-3, Moscow 119991, Russia

ARTICLE INFO

Article history:
Received 3 August 2010
Received in revised form 26 January 2011
Accepted 28 January 2011
Available online 4 February 2011

Keywords:
Hydride
High pressure
$TiCr_2$-based alloys
$ZrFe_2$-based alloys

ABSTRACT

Hydrogen sorption properties of a large variety of solid solutions on the base of $ZrCr_2$ and $TiFe_2$ intermetallic compounds are studied at pressures up to 300 MPa. Partial substitution of Cr by small amounts of Me = Al, Mn, Mo, Ni and B does not significantly change the H/M ratio of hydrides of the $Ti(Cr_{1-x}Me_x)_{2-a}$ alloys with $0 < a < 0.2$, whereas the substitution by Me = Si results in a steep decrease of this ratio. An increase in the concentration of the substituting metal inhibits the transformation of the studied hydrides from the initial Laves phase to a CaF_2-type structure with increasing hydrogen pressure at a temperature of −50 °C. In the case of the $ZrFe_2$ compound, substituting Zr by Dy and Y, and also substituting Fe by V, Cr, Mn, Ni, Cu and Mo decrease the equilibrium absorption and desorption pressures, unlike Ti substitution for Zr and Co substitution for Fe. Substituting Zr by Dy, Y and Ti, as well as substituting Fe by V, Cr, Ni and Cu decrease the hysteresis between the formation and decomposition pressures of the hydrides. In the case of $Zr_{1-x}Ti_x(Fe_{1-y}Me_y)_2$ multicomponent alloys with Me = V and/or Ni, the decomposition pressure varies in a wide range of 0.5–250 MPa. Some of the investigated alloys can be used for designing metal hydride compressors.

1. Introduction

$TiCr_2$ is one of the most interesting IMC among the Laves phases. This compound can crystallise in each of the three AB_2 Laves phase structures: C14, C15 and C36. The reaction of $TiCr_2$ with hydrogen at high pressure and low temperature yields hydride with a cubic CaF_2-type structure. This hydride is a promising material for practical applications because of its high hydrogen storage capacity of 3.6 wt.% [1–3].

Formation of a hydride in the $ZrFe_2$–H_2 system was first reported in ref. [4]. Later, the PC-isotherms and the ΔH (enthalpy) and ΔS (entropy) values for the reaction of $ZrFe_2$ with hydrogen were determined in ref. [5]. At a temperature of 20 °C, this reaction starts at 81 MPa in the first absorption cycle. The equilibrium absorption/desorption pressures for the activated sample are 69.9/32.9 MPa. The hydrogen absorption capacity of $ZrFe_2$ is about 1.7 wt.% and nearly all absorbed hydrogen can be desorbed reversibly, which makes this material a good candidate for practical applications such as metal–hydride compressors.

Studies of non-stoichiometric $ZrFe_x$–H_2 systems showed that their equilibrium hydrogen absorption/desorption pressures increase, whereas the hydrogen storage capacity and desorption enthalpy decrease with increasing iron content [6].

The addition of substituting metals to intermetallic compounds is a commonly used method of changing the thermodynamic parameters of hydrides. An investigation of $Zr_{1-x}R_xFe_2$–H_2 systems with R = Y, Dy and Gd showed that a noticeable solubility of the rare-earth metal could only be achieved for Y and Dy [7]. Alloying $ZrFe_2$ with Y and Dy decreased the equilibrium desorption pressure of hydrogen by 25% and by 10%, respectively, without a considerable loss of the hydrogen storage capacity. In addition to changing the thermodynamics, the rare-earth metals also played a catalytic role in the hydrogen absorption by $ZrFe_2$. For example, the $Zr_{1-x}R_xFe_2$ alloys began to react with hydrogen at a lower pressure than $ZrFe_2$ and without an induction period.

The hydrogen sorption properties of $Zr_{1-x}Ti_xFe_{2-y}Al_y$–H_2 systems ($x = 0.2$–0.8; $y = 0.1$–0.8) were described in our previous work [8]. The results were in good agreement with data of ref. [9] for the $Zr(Fe_{1-x}Al_x)_2$–H_2 systems. The hydrogen storage capacity was found to decrease with increasing content of aluminium and iron. Increasing titanium content of the $Zr_{1-x}Ti_xFe_{2-y}Al_y$ alloys resulted in the increase of the equilibrium absorption and desorption pressures, while both these pressures decreased in the case of aluminium. The hysteresis factor $\ln(P_{abs}/P_{des})$ decreased with increasing content of both Ti and Al metals.

2. Experimental

The initial alloys were arc-melted from pure metals in an argon atmosphere. All samples were remelted 4 times to insure homogeneity. The phase composition and cell parameters of the initial alloys and their hydrides were examined by

* Corresponding author. Tel.: +7 495 9391413; fax: +7 495 9328846.
E-mail address: tim.zotov@gmail.com (T.A. Zotov).

0925-8388/$ – see front matter © 2011 Elsevier B.V. All rights reserved.
doi:10.1016/j.jallcom.2011.01.198

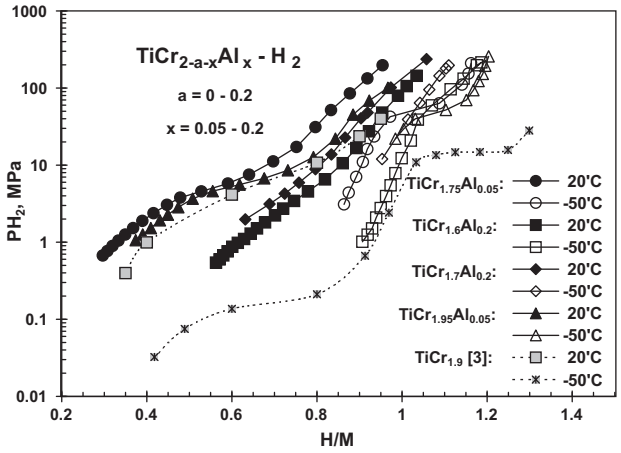

Fig. 1. Desorption PC-isotherms of the $TiCr_{2-a-x}Al_{xx}$–H_2 system at 20 and −50 °C.

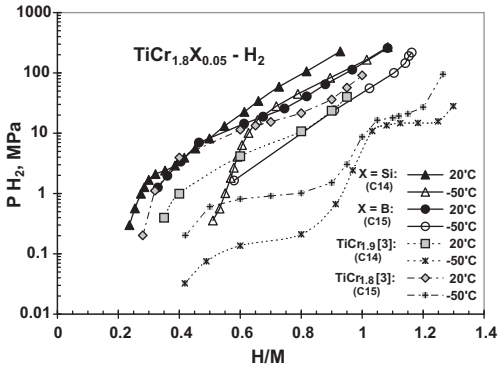

Fig. 2. Desorption PC-isotherms of the $TiCr_{1.8}X_{0.05}$–H_2 system at 20 and −50 °C.

powder X-ray analysis on a DRON-3 M diffractometer with graphite monochromator at room temperature using Cu Kα radiation. Profile refinement was performed using the RIETAN-2000 software [10]. The single-phase alloys were further studied as cast. The multiphase samples were annealed in evacuated quartz tubes at 900 °C for 240 h and quenched in cold water. Hydrogen interaction with the alloys was studied by the PCT-isotherm method in the pressure range of 0.01–300 MPa at temperatures from −50 to 40 °C using a high gaseous pressure device [11]. The amount of the absorbed or desorbed hydrogen was calculated using a modified van der Waals equation [12]. Thermodynamic parameters of the desorption reactions were calculated by the van't Hoff equation using the fugacity values corresponding to the experimental pressure values. A special procedure was employed to prevent hydrogen losses from the hydride phases during their X-ray investigation under ambient conditions. Prior to the X-ray experiments, the samples were first cooled to the liquid nitrogen temperature under high hydrogen pressure and then exposed to air for 5–10 min. Results of the X-ray studies were later used for the adjustment of PCT-calculations so as to take into account the alterations of the sample density during the hydrogenation/dehydrogenation reactions.

3. Results and discussion

3.1. $TiCr_2$-based alloys

We prepared four $TiCr_{2-a-x}Al_x$ alloys with different stoichiometry (Table 1). The hydrogen desorption isotherms of these alloys are shown in Fig. 1. The alloys with $x = 0.05$ and 0.2 and a stoichiometric ratio of B/A = 1.8, as well as the stoichiometric alloy with B/A = 2 and a small concentration of Al ($TiCr_{1.95}Al_{0.05}$) underwent a transformation to a CaF_2-type hydride at −50 °C. An increase of the B/A ratio to 1.9 at $x = 0.2$ prevented from this additional hydrogen absorption.

In the case of the $TiCr_{2-a-x}Mn_x$ alloys with different stoichiometric ratios, the transformation to the CaF_2-type hydride phase at high pressure and low temperature only occurred if $x = 0.2$ and $a = 0.2$, and it was inhibited by increasing x and decreasing a values (Table 1). These results are in good agreement with data for the stoichiometric Ti–Cr–Mn alloys [3,13].

It can therefore be concluded that the partial substitution of Cr by Al and Mn does not significantly change the H/M ratio, whereas the increase of the stoichiometric ratio and the concentration of the substituting metal prevents from the transformation to the CaF_2-type hydride (Table 1).

A study of the effect of B and Si additions to $TiCr_{1.8}$ showed that both elements brought the alloy into multiphase states, with C15 being the main phase in the case of boron and C14 in the case of silicon. The unit cell volume decreased with the addition of these p-elements. The hydrogen desorption pressure increased with the addition of B and decreased with Si (Fig. 2). The H/M ratios decreased in both cases; the decrease with adding Si being steeper. Both boron and silicon hindered the transformation to the CaF_2-type hydride phase, as can be seen from Fig. 2 and Table 1.

The influence of the Cr substitution by Ni was investigated for the $TiCr_{1.75}Ni_{0.1}$ and $TiCr_{1.7}Ni_{0.3}$ compounds (Fig. 3, Table 1). Traces of the Ti_2Ni phase were detected in both alloys even after the annealing. The unit cell volume of the $TiCr_2$ Laves phase and the equilibrium absorption and desorption pressures decreased with increasing Ni content. The H/M values changed insignificantly for $x_{Ni} = 0.1$ and showed a marked decrease for $x_{Ni} = 0.3$ (Fig. 3). Increasing Ni content prevents the formation of the CaF_2-type hydride in the $TiCr_{2-x-a}Ni_x$–H_2 system. In the case of $x_{Ni} = 0.1$, all traces of the C14 phase observed in the X-ray pattern of the initial alloy, completely disappeared after the hydride formation. An X-ray analysis of the hydrogenated sample detected only reflexes corresponding to the C15 and CaF_2-type hydride phases. It is worth noting here that the preparation of single-phase samples of the C15 cubic phase of $TiCr_{\sim 2}$ containing no traces of other Laves phases is a difficult experimental problem [14,15].

The effect of a Mo addition to $TiCr_2$ was studied in the cases of the molybdenum substitution for Ti-atoms ($Ti_{0.86}Mo_{0.14}Cr_{1.9}$) and for Cr-atoms ($TiCr_{1.9}Mo_{0.1}$). The $Ti_{0.86}Mo_{0.14}Cr_{1.9}$ alloy contained a certain amount of a BCC phase even after the annealing (Table 1). The Mo addition was found to decrease both the unit cell volume of the Laves phase and its hydrogen storage capacity. The Mo substitution for Ti increased the equilibrium absorption and desorption pressures. The Mo substitution for Cr gave the opposite effect. The formation of the second (high pressure) plateau was only detected

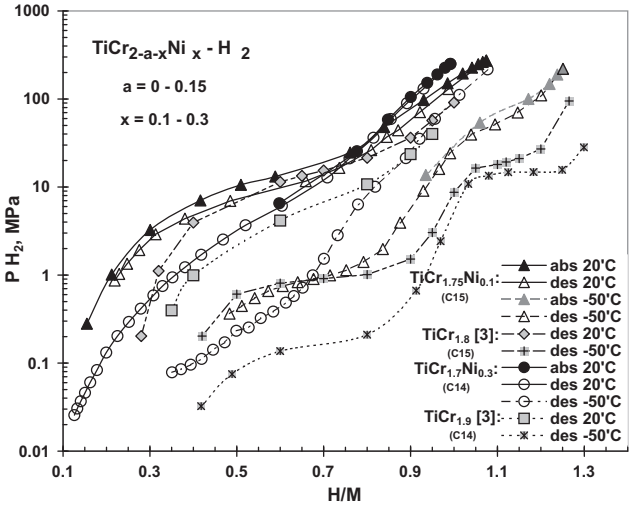

Fig. 3. Absorption and desorption PC-isotherms of the $TiCr_{2-a-x}Ni_x$–H_2 system at 20 and −50 °C.

Table 1
Structure and hydrogen sorption properties of $TiCr_2$-based alloys.

Alloy	Phase composition V_{IMC} (Å^3)	H_2 (wt.%)/H/$M_{20\,^\circ C}$/H_2 (wt.%)/H/$M_{-50\,^\circ C}$[a]	$P_{abs/des\ 20\,^\circ C}$ (MPa)	$\ln(P_a/P_b)$	$P_{abs/des-50\,^\circ C}$[b] (MPa)	P_{des} 90°C calc (MPa)	ΔH (J/mol H_2)/ΔS (J/K mol H_2)[c]
$TiCr_{1.9}$ [3]	C14 168.23	2.0/1.0 2.5/1.3	–/5.4	–	–/14.7	31.4	26.5/122 26/158
$TiCr_{1.8}$ [3]	C15 333.82	2.0/1.0 2.5/1.3	–/15.4	–	–/19.3	56.7	21.3/116 22.6/147
$TiCr_{1.75}Al_{0.05}$	C14 168(5)	1.9/1.0 2.3/1.2	6.08/5.99	0.02	59.8/55.7 0.07	37.5	24/116
$TiCr_{1.6}Al_{0.2}$	C14 168(4)	2.1/1.0 2.4/1.2	1.52/1.42	0.07	–/131.7	29.9	33.4/90.8
$TiCr_{1.7}Al_{0.2}$	C14 169(3)	2.2/1.05 2.3/1.1	2.33/2.23	0.04	–	38.5	28.1/128.5
$TiCr_{1.95}Al_{0.05}$	C14 168(7)	2.1/1.0 2.4/1.2	10.64/2.94	1.29	–/48.1	30.7	22.8/112 24.8/167
$TiCr_{1.6}Mn_{0.2}$	C14 166.5(2)	1.9/0.95 2.4/1.2	6.28/6.08	0.03	20.3/–	43.9	28.0/129
$TiCr_{1.7}Mn_{0.3}$	C14 165(4)	2.05/1.05 2.4/1.2	6.59/3.95	0.51	–	–	–
$TiCr_{0.95}Mn_{0.95}$	C14 165(2)	2.0/1.05 2.2/1.15	15.91/8.82	0.59	–	43.0	22.8/114.9
$TiCr_{1.8}B_{0.05}$	C15 82% 333.618(9) C14 16% 167.01(6) bcc 2% 28.75	2.1/1.05 2.2/1.1	22.3/18.8	0.17	–	41.0	15.6/94.8
$TiCr_{1.8}Si_{0.05}$	C14 166.26(3)	1.8/0.95 2.1/1.25	3.34/3.24	0.03	–/99.3	15.7	21.4/101 10.9/113
$TiCr_{1.75}Ni_{0.1}$	C15 75% 332.15(2) C14 18% 165.92(8) Ti_2Ni 8% 1455.7(4)	2.1/1.1 2.4/1.25	14.19/10.13	0.34	60.8/42.6 0.36	39.5	20.5/107.8 25.5/167
$TiCr_{1.7}Ni_{0.3}$	C14 89%165.636(5) Ti_2Ni 5% 1453.3(3) bcc(Cr)6%24.693(2)	1.9/1.0 2.1/1.05	6.59/4.86	0.30	–	25.3	21.7/106.7
$Ti_{0.86}Mo_{0.14}Cr_{1.9}$	C15 86%330.73(3) bcc 14% 25.16(2)	1.9/1.0	83.09/77.00	0.08	–	175.9	17.2/117
$TiCr_{1.9}Mo_{0.01}$	C14 166(5)	1.9/1.0 2.2/1.15	11.65/3.55	1.19	60.8/27.4 0.8	21.7	24.8/113

[a] Hydrogen absorption capacity at high pressure (1000–3000 atm) and at 20 °C/and at high pressure (1000–3000 atm) and at −50 °C.
[b] The values of hydrogen absorption/desorption pressures of the second plateau (CaF_2 type hydride forming/decomposition).
[c] The second pares of enthalpy and entropy values correspond to the second plateau in PC-isotherms (CaF_2 type hydride decomposition reaction).

in the $TiCr_{1.9}Mo_{0.1}$–H_2 system (Fig. 4). However, an X-ray analysis of the sample of $Ti_{0.86}Mo_{0.14}Cr_{1.9}$ hydride showed traces of the CaF_2-type phase.

3.2. $ZrFe_2$-based alloys

To investigate the effect of a Ti substitution for Zr, we studied the $Zr_{1-x}Ti_xFe_2$ alloys with $x = 0.2$ and 0.4 (Table 2). The $Zr_{0.8}Ti_{0.2}Fe_2$ compound had a C15 structure similar to that of $ZrFe_2$, whereas $Zr_{0.6}Ti_{0.4}Fe_2$ was a mixture of 60% C14 and 40% C15 Laves phases. The amount of these phases did not significantly change after the annealing, because the composition of the sample belonged to the two-phase (C14 + C15) region of the Zr–Ti–Fe phase diagram [16]. The lattice parameters decreased with increasing titanium content (Table 2). The increase of the Ti content also resulted in the drastic increase of the equilibrium absorption and desorption pressures, while the hysteresis between these pressures decreased and the hydrogen storage capacity decreased, too (Fig. 5, Table 2). The maximum hydrogen capacity was achieved for the hydride $Zr_{0.6}Ti_{0.4}Fe_2H_{2.9}$ loaded with hydrogen at a temperature as low as −40 °C.

All $ZrFe_{1.8}Me_{0.2}$ alloys (Me = V, Cr, Mo, Mn, Co, Ni, Cu) had C15 type structures except for the alloys with V (a mixture of C15 + C14) and Mo (C14). The unit cell volume of the C15 phase decreased in the series V to Ni and increased for the Cu-substituted alloy. The hydrogen content was almost the same (~1.75 wt.%) for all studied systems. The dependence of the equilibrium absorption/desorption pressures on the atomic number of the substituting metal is shown in Fig. 6. The equilibrium pressures are maximal in the case of the alloy with Co (P_{abs}/P_{des} = 73.5/36.7 MPa). A similar increase of the plateau pressures was found in the case of Co substituting for Fe in

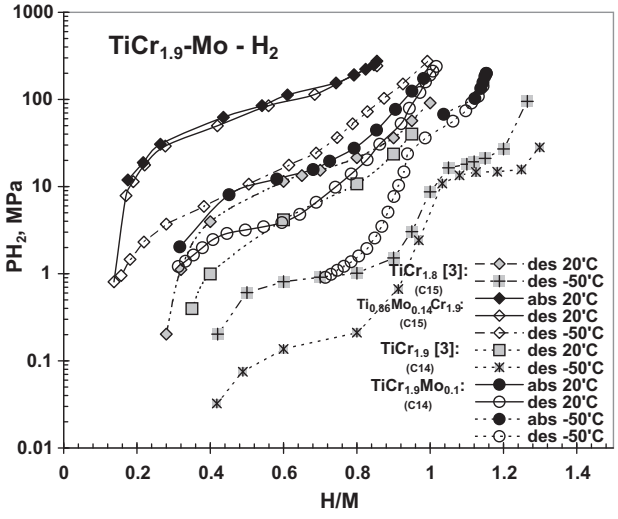

Fig. 4. Absorption and desorption PC-isotherms of the $TiCr_{1.9}$–Mo–H_2 system at 20 and −50 °C.

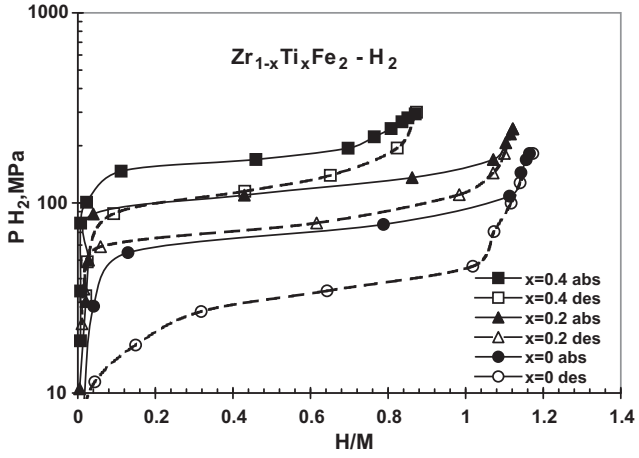

Fig. 5. Absorption and desorption PC-isotherms of the $Zr_{1-x}Ti_xFe_2$–H_2 system at 20 °C.

Table 2
Structure and hydrogen sorption properties of $ZrFe_2$-based alloys.

Alloy	Phase composition, V_{IMC} (Å^3)	$\Delta V/V$, %	H_2 (wt.%)/H/M[a]	$P_{abs/des\ 20\,^\circ C}$ (MPa)	$\ln(P_a/P_d)$	P_{des} 90 °C, calc (MPa)	ΔH (kJ/mol H_2)/ΔS (J/K mol H_2)
$ZrFe_2$ [5]	C15 352.46	24.3	1.7/1.18	69.9/32.9	0.75	112.1	21.3/121
$Zr_{0.9}Y_{0.1}Fe_2$ [7]	C15 353.2(5)	–	1.7/1.13	39.5/25.9	0.42	98.6	21.5/121
$Zr_{0.8}Ti_{0.2}Fe_2$	C15 348.02	24.2	1.8/1.16	117.5/76.5	0.43	200.7	20.7/129
$Zr_{0.6}Ti_{0.4}Fe_2$	C15 41% 342.05(3)	22.8	1.54/0.87	168.2/115.5	0.38	283.0	20.6/135
	C14 58% 165.67(5)	23.8					
$ZrFe_{1.8}V_{0.2}$	C15 68% 354.59(3)	24.8	1.8/1.2	1.57/1.22	0.26	7.90	23.6/102.5
	C14 32% 178.83(7)	24.8					
$ZrFe_{1.8}Cr_{0.2}$	C15 353.94(2)	23.9	1.75/1.21	7.90/5.47	0.37	26.9	22.3/109
$ZrFe_{1.8}Mo_{0.2}$	C14 179.22(3)	23.6	1.6/1.18	6.38/1.93	1.20	13.5	25.9/112.5
$ZrFe_{1.8}Mn_{0.2}$	C15 353.74(2)	28.0	1.8/1.21	29.5/14.29	0.72	60.3	21.8/115.8
$ZrFe_{1.8}Co_{0.2}$	C15 352.763(4)	22.7	1.7/1.18	73.5/36.7	0.69	101.3	16.8/108.1
$ZrFe_{1.8}Ni_{0.2}$	C15 351.03(2)	24.2	1.7/1.18	46.1/25.33	0.60	92.2	21.5/119.7
$ZrFe_{1.8}Cu_{0.2}$	C15 352.03(1)	25.0	1.65/1.12	32.8/21.99	0.40	74.0	19.6/112
$Zr_{0.3}Ti_{0.7}Fe_{1.4}V_{0.6}$	C14 170.35(1)	18.0	2.1/1.18	0.51/0.42	0.20	4.0	31.1/116
$Zr_{0.2}Ti_{0.8}Fe_{1.6}V_{0.4}$	C14 165.088(1)	20.6	1.8/0.99	17.23/16.52	0.04	60.3	19.7/109.9
$Zr_{0.1}Ti_{0.9}Fe_{1.7}V_{0.3}$	C14 161.47(2)	22.2	1.8/0.98	139.8/129.7	0.08	249.5	13.5/112.9
$Zr_{0.6}Ti_{0.4}Fe_{1.2}Ni_{0.8}$	C15 331.44(3)	24.6	1.64/1.02	161.1/147.9	0.09	290.8	16.5/124
$Zr_{0.8}Ti_{0.2}FeNi_{0.8}V_{0.2}$	C15 343.69(1)	25.0	1.9/1.23	2.89/2.79	0.04	19.8	26.8/118.3
$Zr_{0.1}Ti_{0.9}Fe_{1.5}Ni_{0.3}V_{0.2}$	C14 160.042(9)	20.4	1.8/0.99	–/256.4	0.08_{-20C}	408.8	12.08/119.5

[a] Hydrogen absorption capacity at high pressure (1000–3000 atm) at 20 °C.

$ZrFe_2$ [17]. The hysteresis factor $\ln(P_{abs}/P_{des})$ is the highest for pure $ZrFe_2$.

The decrease of the equilibrium hydrogen pressure due to alloying $ZrFe_2$ with Ni looks rather surprising. In fact, alloying $ZrFe_2$ with V, Cr, Mn, Fe and Co decreases its unit cell volume (Table 2, Fig. 6), while the absorption and desorption pressures increase. The unit cell volume of $ZrFe_{1.8}Ni_{0.2}$ is the lowest in this series. Correspondingly, the equilibrium pressures for the Ni-substituted alloy should be higher than that for the Co-substituted alloy. This decrease can be accounted for by the nature of the Ni–H chemical bonding, because the formation enthalpy of the binary hydrides increases in the series of 3d-metals from vanadium to cobalt and slightly decreases for Ni [18]. It should be mentioned, however, that our results contradict data of ref. [19] to say that the equilibrium absorption pressure of hydrogen in the $Zr(Fe_{1-x}Ni_x)_2$–H_2 systems increases from 0.4 MPa at $x = 0.2$–0.8 MPa at $x = 0.8$. However, results obtained in ref. [19] do not agree well with the high value of 70 MPa of the hydrogen absorption pressure established for the parent $ZrFe_2$–H_2 system [4,5,17]. We think this contradiction needs further clarification since it is rather unlikely that the substitution of Fe by 0.2 atoms of Ni leads to the strong reduction in pressure from 70 to 0.4 MPa, whereas the further increase of the nickel concentration leads to a slight rise of the hydrogen absorption pressure from 0.4 to 0.8 MPa.

The influence of substituting metals on the hydrogen sorption properties of $ZrFe_2$ can be summarised as follows. The increase of the equilibrium absorption and desorption pressures occurs in the case of the Ti substitution for Zr and Co substitution for Fe. The opposite effect is observed for the Zr substitution by Dy and Y and Fe substitution by V, Cr, Mn, Ni, Cu. A partial replacement of Zr by Dy, Y, Ti and Fe by V, Cr, Ni, Cu leads to the decrease of the hysteresis factor.

A study of the $Zr_{1-x}Ti_x(Fe_{1-y}Me)_2$ alloys with Me = V, Ni showed that the hydrogen absorption and desorption pressures of relevant hydrides vary on a broad scale (Fig. 7, Table 2). The highest desorption pressure of 256 MPa at 20 °C and the lowest desorption enthalpy of 12 kJ/mol H_2 among all systems studied in this work was observed for the $Zr_{0.1}Ti_{0.9}Fe_{1.5}Ni_{0.3}V_{0.2}$–$H_2$ system. The com-

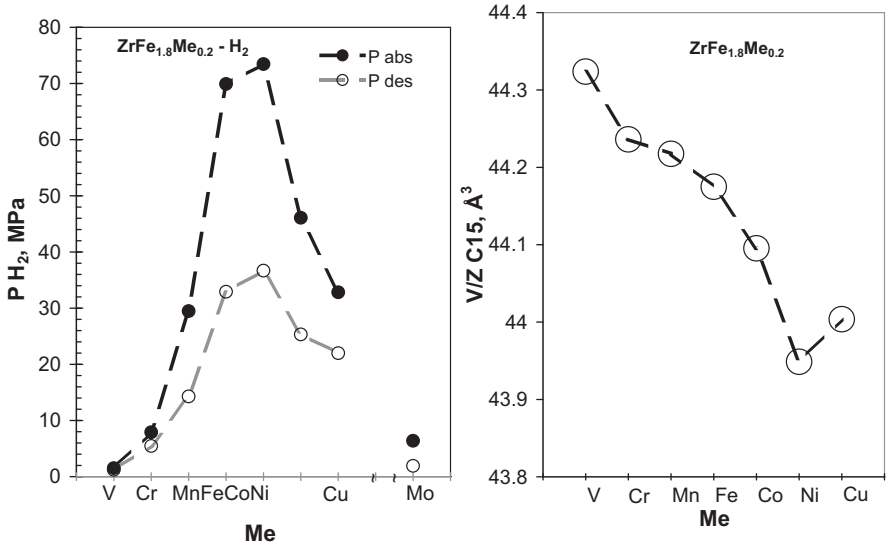

Fig. 6. The influence of substituting metal Me on the hydrogen absorption–desorption pressures at 20 °C and the unit cell volume of the $ZrFe_{1.8}Me_{0.2}$ system.

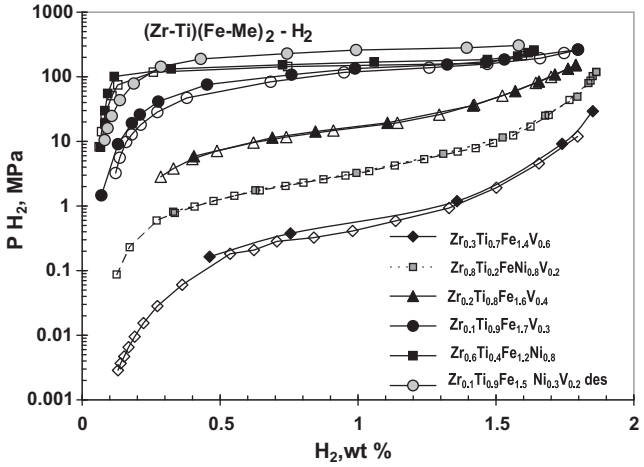

Fig. 7. The absorption (filled marks) and desorption (opened marks) PC-isotherms of the. (Zr–Ti)(Fe–Me)$_2$–H_2 system at 20 °C.

plete saturation of the corresponding hydride is possible only at a temperature below −20 °C and a pressure of 300 MPa. The desorption pressure at 90 °C was calculated using the van't-Hoff equation (Table 2).

The obtained results provide the possibility to forecast the hydrogen equilibrium absorption and desorption pressures for more complicated systems, such as $(Zr_{1-x}M'_x)(Fe_{1-y}M''_y)_2$ (M′ = Ti, Y, Dy; M″ = V, Cr, Mn, Co, Ni, Cu, Mo), based on Vegard's law. The accuracy of these predictions strongly depends on the homogeneity and phase composition of the initial alloys, whose thermodynamic parameters were chosen as database entries.

The hydrides synthesised in this study are rather perspective for practical applications such as metal–hydride compressors. Using the data from Tables 1 and 2, it is possible to select pairs of alloys, which can provide a 4-stage compression of hydrogen from 0.5 to 100 MPa utilising cold and waste hot water as the heat-transfer agents.

4. Conclusions

Hydrogen sorption properties of $Ti_{1-a}Cr_{2-b}Me_c$ (Me = Al, Mn, Mo, Ni, B, Si) alloys were studied in the present work. The substitution of Cr by small amounts of Al, Mn, Mo, Ni and B did not significantly change the hydrogen absorption capacity in contrast to the Si-substitution. Increasing concentration of the substituting metal and the stoichiometry ratio prevents from the formation of higher hydrides with the CaF_2-type structures. Stabilization of the CaF_2-type hydrides can be achieved by introducing "hydride-forming" metals like V (in this case, the initial alloy will have a BCC structure instead of the Laves phase [20]).

The addition of other elements gives the opportunity to vary the thermodynamics of $ZrFe_2$ hydride. The multicomponent $(Zr_{1-x}M'_x)(Fe_{1-y}M''_y)_2$ (M′ = Ti, Y, Dy; M″ = V, Cr, Mn, Co, Ni, Cu, Mo) alloys are characterised by a wide range of the absorption and desorption pressures (0.5–250 MPa) and desorption enthalpies (12–31 kJ/mol H_2), and low hysteresis factors $\ln(P_{abs}/P_{des}) = 0.04–0.2$. These results provide a good perspective for practical application of the studied hydrides in metal–hydride compressors.

Acknowledgements

The authors would like to acknowledge Dr. V. Antonov for valuable discussion.

This work was supported in part by General Motors Corp and Russian Foundation for Basic Research (Grant No. 10-03-00883).

References

[1] J.R. Johnson, J.J. Reilly, F. Reidinger, L.M. Corliss, J.M. Hastings, J. Less-Common Met. 88 (1982) 107–114.
[2] S.N. Klyamkin, V.F. Demidov, V.N. Verbetsky, Rus. Vestn. MGU, ser. 2. Himia. 34–4 (1993) 412–416.
[3] O. Beeri, D. Cohen, Z. Gavra, M.H. Mintz, J. Alloys Compd. 352 (2003) 111–122.
[4] S.M. Filipek, I. Jacob, V. Paul-Boncour, A. Percheron-Guegan, I. Marchuk, D. Mogilyanski, J. Pielaszek, Pol. J. Chem. 75 (2001) 1921–1926.
[5] T. Zotov, E. Movlaev, S. Mitrokhin, V. Verbetsky, J. Alloys Compd. 459 (2008) 220–224.
[6] R.B. Sivov, T.A. Zotov, V.N. Verbetsky, Hydrogen sorption properties of ZrFex ($1.9 \le x \le 2.5$) alloys, Int. J. Hydrogen Energy 36 (2011) 1355–1358.
[7] R.B. Sivov, T.A. Zotov, V.N. Verbetsky, The influence Y, Gd and Dy doping on hydrogen sorption properties of $ZrFe_2$, in: A.A. Yukhimchuk (Ed.), Interaction of Hydrogen Isotopes with Structural Materials (IHISM-08 Junior), Sarov, 2009, pp. 201–208.
[8] R.B. Sivov, T.A. Zotov, V.N. Verbetsky, Inorg. Mater. 46 (N 4) (2010) 372–376.
[9] M. Bereznitsky, I. Jacob, J. Bloch, M.H. Mintz, J. Alloys Compd. 351 (2003) 180–183.
[10] F. Izumi, J. Rigaku. 17–1 (2000) 34–45.
[11] S. Mitrokhin, T. Zotov, E. Movlaev, V. Verbetsky, J. Alloys Compd. 446–447 (2007) 603–605.
[12] H. Hemmes, A. Driessen, R. Griessen, J. Phys. C: Solid State Phys. 19 (1986) 3571–3585.
[13] F. Agresti, S. Lo Russo, A. Maddalena, G. Principi, G. Mazzolai, B. Coluzzi, Mater. Sci. Eng. A 521–522 (2009) 143–146.
[14] O. Beeri, D. Cohen, Z. Gavra, J.R. Johnson, M.H. Mintz, J. Alloys Compd. 267 (1998) 113–120.
[15] O. Beeri, D. Cohen, Z. Gavra, J.R. Johnson, M.H. Mintz, J. Alloys Compd. 293–295 (1999) 14–18.
[16] G. Zhou, D. Zeng, Z. Liu, J. Alloys Compd. 490 (2010) 463–467.
[17] S.M. Filipek, V. Paul-Boncour, N. Kuriyama, N. Takeichi, H. Tanaka, R.-S. Liu, R. Wierzbicki, R. Sato, H.-T. Kuo, Solid State Ionics 181 (2010) 306–310.
[18] B.A. Kolachev, et al., Gidridnye Sistemy, Metallurgiya, Moscow, 1992, p. 230.
[19] A. Jain, R.K. Jain, S. Agarwal, V. Ganesan, N.P. Lalla, D.M. Phase, I.P. Jain, Int. J. Hydrogen Energy 32 (2007) 3965–3971.
[20] M. Enomoto, J. Phase Equilib. 13–2 (1992) 195–200.